J. exp. Biol 117, 87–110 (1985)
Printed in Great Britain © *The Company of Biologists Limited 1985*

THE ULTRASTRUCTURE OF THE EPICUTICULAR INTERFERENCE REFLECTORS OF TIGER BEETLES (*CICINDELA*)

BY T. D. SCHULTZ AND M. A. RANKIN
Department of Zoology, University of Texas, Austin, Texas 78712, U.S.A.

Accepted 4 December 1984

SUMMARY

Tiger beetles of the genus *Cicindela* exhibit iridescent structural coloration due to the presence of a non-ideal multilayer interference reflector located in the outermost 2 μm of the integument. The reflector is composed of alternating layers of electron-lucent and electron-dense material. This series of layers was distinguished from chitinous procuticle by its position, ultrastructure and solubility in dilute KOH. The reflector appears homologous with the inner epicuticle of current models. Measurements of surface reflectance, refractive index and the dimensions of the alternating layers suggests that the dense layer has a refractive index (RI) near 2·0 and may be a melanoprotein.

INTRODUCTION

The widespread occurrence of structural coloration in insect cuticle received vigorous attention in the early part of this century (Biederman, 1914; Onslow, 1920; Mason, 1927). These researchers ascribed the physical colours of the integument to the constructive interference of light reflected from thin layers within the exoskeleton. However, the exact anatomy of the reflector remained obscure, and proposals of morphologies varied widely. The advent of the electron microscope finally allowed ultrastructural studies of cuticular reflectors. The bulk of this work focused on interference reflectance by specialized structures such as insect cornea and lepidopteran wing scales (Bernard & Miller, 1968; Ghiradella *et al.* 1972). However, the most complete study of interference reflectance by whole cuticle was Neville & Caveney's (1969) work on scarab beetles. While that work elegantly described the exocuticular reflectors within that family, the morphologies of cuticular reflectors in other metallic-coloured insects have remained undescribed.

Coincidental with the early work on insect coloration, several authors described the elytral structure of several groups of beetles which exhibit interference reflectance (Buprestidae; Hass, 1916; Cicindelidae: Stegemann, 1930; Carabidae: Sprung, 1931). Stegemann (1930) described a superficial layer, the 'Sekretschicht', in tiger beetles (Cicindelidae) which dissolves in dilute KOH at 60 °C and pours from secretory glands after ecdysis. Mandl (1931) later ascribed the iridescence of *Cicindela* to

Key words: Interference colour, epicuticle, *Cicindela*.

this 'Sekretschicht'. Shelford (1917) independently suggested that a surface film reflects interference colours in *Cicindela*.

Many of the elytral structures described by early histological and morphological studies have not been re-examined rigorously under current concepts of cuticle structure. However, homologies have been proposed for these structures based upon more recent research involving other cuticles. Wigglesworth (1972) suggested that the 'Sekretschicht' may be analogous to the cement layer of other insects. Richards (1951) preferred the term 'tectocuticle' for this outermost layer presumed to be secreted by the dermal glands. A recent electron microscope study by Mossakowski (1980) identified an interference reflector in the outermost layers of cuticle in *Cicindela campestris*. He identified the reflective cuticle as exocuticle.

The following study attempts to locate the multilayer reflective system of cicindelid cuticle, to describe its ultrastructure, and to determine to what extent this cuticle conforms to the current models of insect morphology.

MATERIALS AND METHODS

Reflection from elytral surfaces was measured using a Cary 17D spectrophotometer. Elytra for reflectance measurements were taken from four species of tiger beetles, *Cicindela formosa* Say, *C. splendida* Hentz, *C. scutellaris rugata* Dejean and *C. repanda* Dejean. Adults of all four species were collected at Bastrop State Park, Bastrop County, Texas.

Samples of adult cuticle were cut or torn from the elytra and thoraces, and subjected to a variety of chemical treatments. They were then prepared for either scanning or transmission electron microscopy.

Chemical treatments of cuticle

In order to differentiate the epicuticle from the exocuticle, fragments of cuticle were immersed in 8 % KOH at 60 °C for periods of 4, 9, 12, 24, 48 h and 6 days. One set of samples was treated with concentrated KOH for 15 min at 160 °C. A second set was treated similarly, but followed with a 17-h immersion in 8 % KOH. Treatment with hot concentrated alkali is the initial step in the chitosan method of Campbell (1929) for detection of chitinous cuticle. All samples were rinsed with distilled water, dried, and any colour or gross textural change observed with a dissecting microscope. The fragments were cut to smaller size and prepared for either scanning or transmission electron microscopy.

In order to remove procuticular layers, elytra were immersed in concentrated H_2SO_4 for 1, 12, 24, 48 and 72 h. The elytra were rinsed with distilled water, dried, and any colour changes noted. The elytral fragments were then prepared for scanning electron microscopy (SEM).

Since H_2O_2 will bleach melanin and alter the interference colours if melanin is one component of the interference reflector, the role of melanin in cicindelid coloration was investigated by treating *C. formosa* and *C. scutellaris* elytral fragments for 6 days with 10 % H_2O_2 at 26 °C. When no colour change was observed, the samples were treated for a seventh day at 60 °C. Samples were dried, observed and prepared for transmission electron microscopy.

Preparation of cuticle for scanning or transmission electron microscopy

Dried strips of treated or untreated cuticle were mounted on edge, sputter-coated with 2·5 nm of gold-palladium, and examined with a Hitachi scanning electron microscope. This orientation provided a view of the torn edge perpendicular to the elytral surface with each cuticle layer exposed in relief.

For transmission electron microscopy, treated and untreated samples of cuticle were cut into extremely fine slivers (0·3 × 1 mm) with a tapering edge. Cuts were positioned between elytral tracheae to avoid trapped air bubbles. The cuticle was fixed in 2·5 % gluteraldehyde and post-fixed in 2 % OsO_4 for 2 h, dehydrated in a standard ethanol and propylene oxide series, and infiltrated in a long series of propylene oxide/Epon-Araldite mixes. Each infiltration step required agitation, and the final two immersions in pure Epon-Araldite were evacuated completely.

Thin sections were cut perpendicular to the elytral surface. Some sections from each treatment group were post-stained for 5 min in 1 % uranyl acetate in 50 % ethanol, followed by 5 min in lead citrate. Portions of the dorsal surface of *C. scutellaris* were also sectioned parallel to the plane of the elytral surface. All sections were examined under a Zeiss 10CA transmission electron miscroscope.

Thin sections of samples from each treatment group were mounted and reserved for interference and polarized light microscopy.

RESULTS

Elytral reflectance

The elytra and thorax of *C. formosa* are deep metallic red with white maculations – peak reflectance occurring at 655 nm, with a secondary peak near 360 nm (Fig. 1A). The Bastrop population of *C. formosa* exhibits the elytral coloration of the race *C. formosa pigmentosignata* Horn. While the maculae of Bastrop individuals are rarely reduced, many individuals exhibit a distal deep purple coloration on the elytron, which is characteristic of *C. formosa pigmentosignata* (Gaumer, 1977). For reflectance measurements and electron microscope studies, elytral fragments were selected from elytral areas which were homogeneously red.

The elytra of *C. splendida* are metallic brick red with a metallic green border. An elytron with the border removed shows maximal reflectance near 635 nm, with a very small secondary peak at 410 nm (Fig. 1B).

C. scutellaris rugata elytra reflect maximally at 499 nm in a relatively narrow band (Fig. 1C). *C. scutellaris* varies greatly in colour among its races, with *rugata* displaying an iridescent blue-green coloration. Both the intensity and the purity of this reflected colour exceed those of *C. formosa* and *C. splendida*.

The brown *C. repanda* elytron has a very different reflectance curve (Fig. 1D). Instead of a sharp peak in the visible wavelengths, the reflectance increases steadily towards the near-infrared.

The colour of tiger beetle elytra, like all interference colours, changes with the angle of viewing. As the angle of reflectance departs from the angle of incidence, the reflected wavelengths become shorter. The elytra of *Cicindela* are alveolate (Fig. 2)

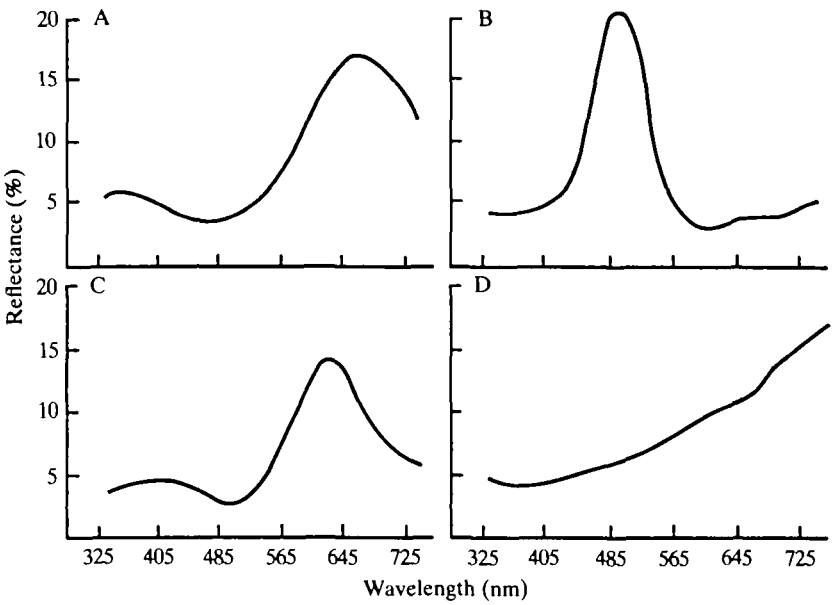

Fig. 1. Reflectance curves of four species of *Cicindela*. (A) *C. formosa pigmentosignata*, (B) *C. scutellaris rugata*, (C) *C. splendida* and (D) *C. repanda*.

with small ($10 \times 10\ \mu m$) hexagonal depressions. The alveoli are superimposed upon larger irregularities in the upper portion of the elytron. Light reflected from this surface is a composite of wavelengths reflected from a variety of angles. Not only would the total intensity of reflection be diminished, but the peak reflectance would be less sharply defined. Of the four species, *C. scutellaris* displays the most regular elytral surface with smooth, shallow alveoli. *C. repanda* and *C. splendida* possess the deepest alveoli and most acute ridges.

Elytral ultrastructure

The general features of elytral structure observed under SEM were consistent in the four species. Above the tracheae, the procuticular layers (region *D* in Fig. 2) are organized in the pseudo-orthogonal 'plywood' fashion that has been described for other Coleoptera (Hepburn, 1972). This region has been defined as endocuticle (Zelazny & Neville, 1972) or as mesocuticle (Hepburn, 1972), and is considered to be untanned or non-sclerotized.

Observed under the SEM, the outermost layer of *Cicindela* cuticle appears as a dense, solid material which bears the alveolate microsculpture of the integument (region *AB* in Fig. 2). This layer ranges in thickness from $3{\cdot}5\ \mu m$ at the bottom of a cell, to $7{\cdot}0\ \mu m$ at the top of an adjacent ridge. The torn vertical face of this layer appears less fibrous and more granular than the underlying cuticle (region *D* in Fig. 2). Occasionally, samples will tear obliquely and reveal two distinct portions of the outer layer in relief (Fig. 3). In these torn samples, a regular banding or lamination of 6–8 extremely even bands (150–200 nm thick) is visible in the outer $1–2\ \mu m$ of the layer (region *A* in Fig. 3B). These laminations appear in contrast to the rougher, non-laminated face of the inner portion (region *B* in Figs 3B and 4). Based upon their

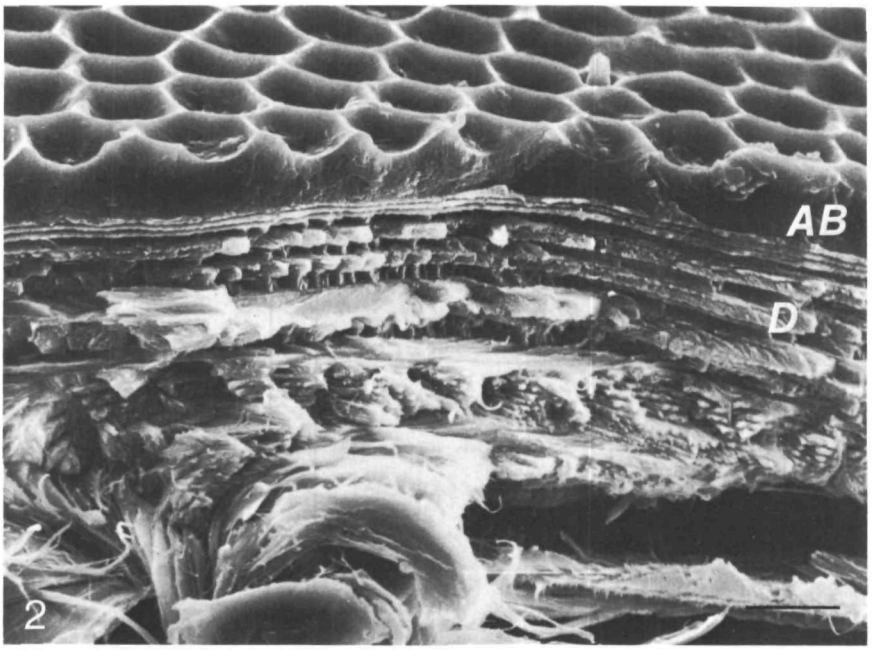

Fig. 2. Scanning electron microscope cross-section of exposed cuticular layers in the upper elytron of *Cicindela splendida*. Region *D* represents the pseudo-orthogonal procuticle. The composite layer *AB* (the presumptive epicuticle and exocuticle) conforms to the alveolate microsculpture of the elytral surface. Scale bar, 10 μm.

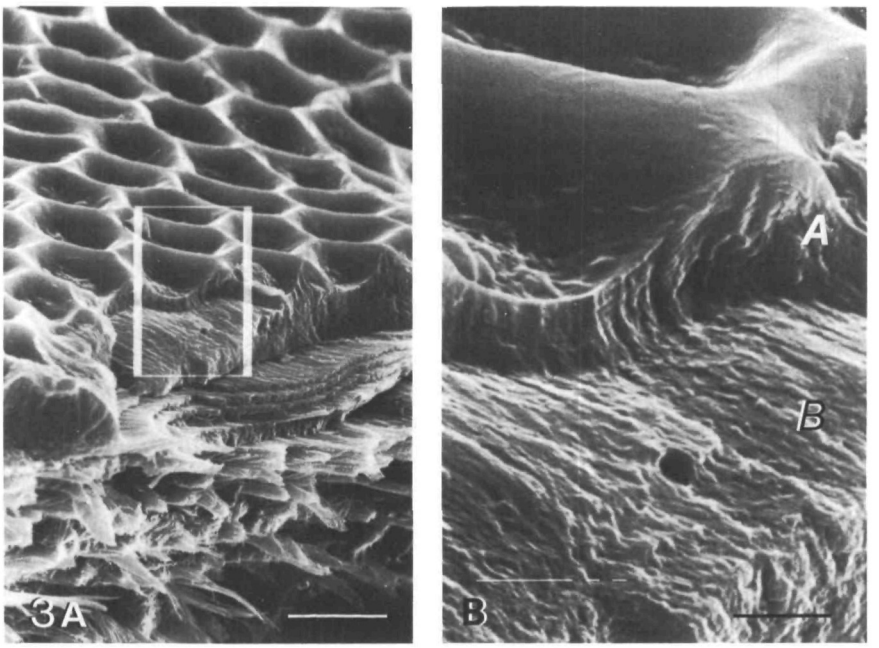

Fig. 3. Layer *A* (presumptive epicuticle) exposed separately from layer *B* (exocuticle). Horizontal laminations are visible in layer *A*. Scale bars: A, 10 μm; B, 2 μm.

ultrastructure, location, development and reaction to solvents, the outer and inner portions of the outer cuticle (layers *A* and *B* in Fig. 4) are here designated the epicuticle and outer exocuticle, respectively, and will be referred to as such throughout this report.

Dermal gland canals measure 0·8 μm in diameter and their orifices are distributed regularly over the surface of the elytron (Fig. 4, *dc*). The pattern of lamination is not disrupted around the canal opening. Epicuticular thickness is enhanced on the ridges, compared to the basins of the alveoli, but is not greater at the dermal gland opening than on adjacent ridges.

Transmission electron microscopy (TEM) reveals that the alveolate superficial layer of the scanning electron micrograph is indeed a composite of two complex layers (layers *A* and *B* in Fig. 5). Immediately below this composite, lie 2–3 thin exocuticular layers (layer *C* in Figs. 5, 6A) which exhibit the distinct arciform appearance of helocoidal cuticle as described by Bouligand (1972).

The outer exocuticle (layer *B* in Fig. 5) appears more electron-dense than the helicoidal or preferred layers below. This layer consists of 25–35 densely packed lamellae ranging in width from 0·055 to 0·1 μm. In some areas, electron-dense granules lie between or within lamellae. In post-stained sections, the horizontal lamellae are resolved into alternate patterns of microfibrils viewed in perpendicular and transverse orientations (Fig. 6B). This pattern closely resembles the description of the non-perfect helicoidal outer exocuticle of *Tenebrio* given by Filshie (1982).

Pore canals, 50–70 nm in diameter, traverse the outer exocuticle (Fig. 6C, *pc*). Within the exocuticle, they appear as segments of tubes containing material much denser than the surrounding fibrils. The pore canals extend into the epicuticle but appear much narrower in diameter (Fig. 6C, arrow). This pattern is similar to the branching of epicuticular filaments described in other insect cuticles (Filshie, 1982).

The epicuticle (Fig. 6D) is composed of a series of extremely dense bands (*D*) between 0·03 and 0·1 μm thick, regularly spaced by electron-lucent bands (*L*) of 0·06–0·125 μm. Each pair of electron-dense and electron-lucent layers corresponds to a single band observed in relief in the scanning electron micrographs. The number of bands varies between four dense layers at the base of a depression to nine layers within an adjacent ridge. Under high magnification, electron-dense layers appear to be composed of vertically aligned granules (Fig. 6D). Post-staining enhances this appearance. The electron-lucent bands exhibit no apparent ultrastructure. The outermost layer is always electron-lucent and 20–30 nm thicker than the other light bands. The outer 20–30 nm appears as a faint shadow of higher density, possibly representing a cuticulin layer (Fig. 6E, *cu*). Mossakowski (1980) identified the outer series of electron-dense and electron-lucent bands as exocuticle. He concluded that the banding was a diffraction pattern resulting from the structural organization of exocuticular fibrils.

Although there are occasional distortions, the organization of the epicuticular layers is exceedingly regular. One individual *L* or *D* layer may vary in thickness horizontally within a section. This is usually an artifact resulting from the section passing obliquely through the layer as it conforms to the alveolate surface. Each *L* or *D* layer may differ slightly in thickness from other *L*/*D* layers in that region of the stack. In *C. scutellaris*, the peripheral dense band is typically fragmented

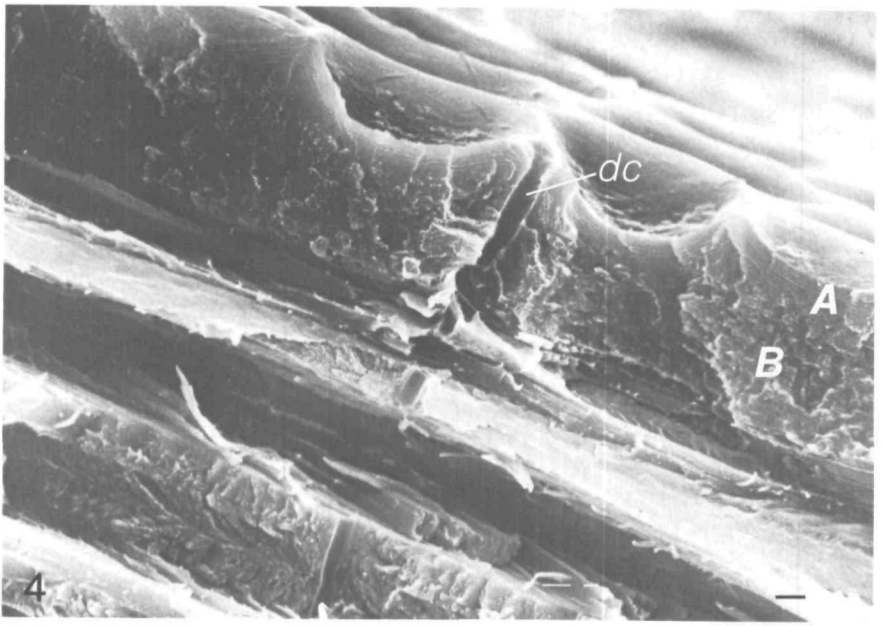

Fig. 4. Scanning electron microscope cross-section of the upper cuticular layers in *Cicindela splendida*. The laminated structure of layer *A* (presumptive epicuticle) distinguishes it from region *B* (presumptive outer exocuticle). *dc*, dermal gland canal. Scale bar, 1 μm

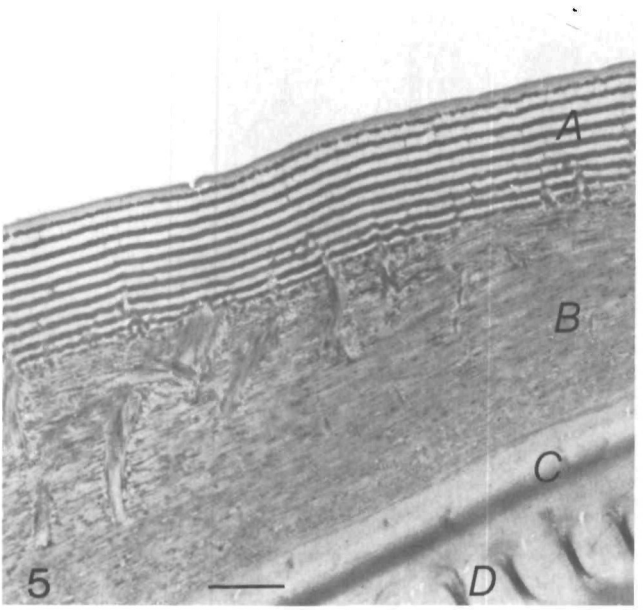

Fig. 5. Transmission electron microscope cross-section of the presumptive epicuticle (*A*) and the outer exocuticle (*B*) in the elytron of *Cicindela scutellaris*. Between the outer exocuticle and the underlying procuticle (*D*), lies a thin layer of helicoidal cuticle (*C*). Scale bar, 1 μm.

and particulate. Partially formed bands occur regularly at the outer exocuticular border.

When the honeycombed surface is sectioned horizontally, the section passes

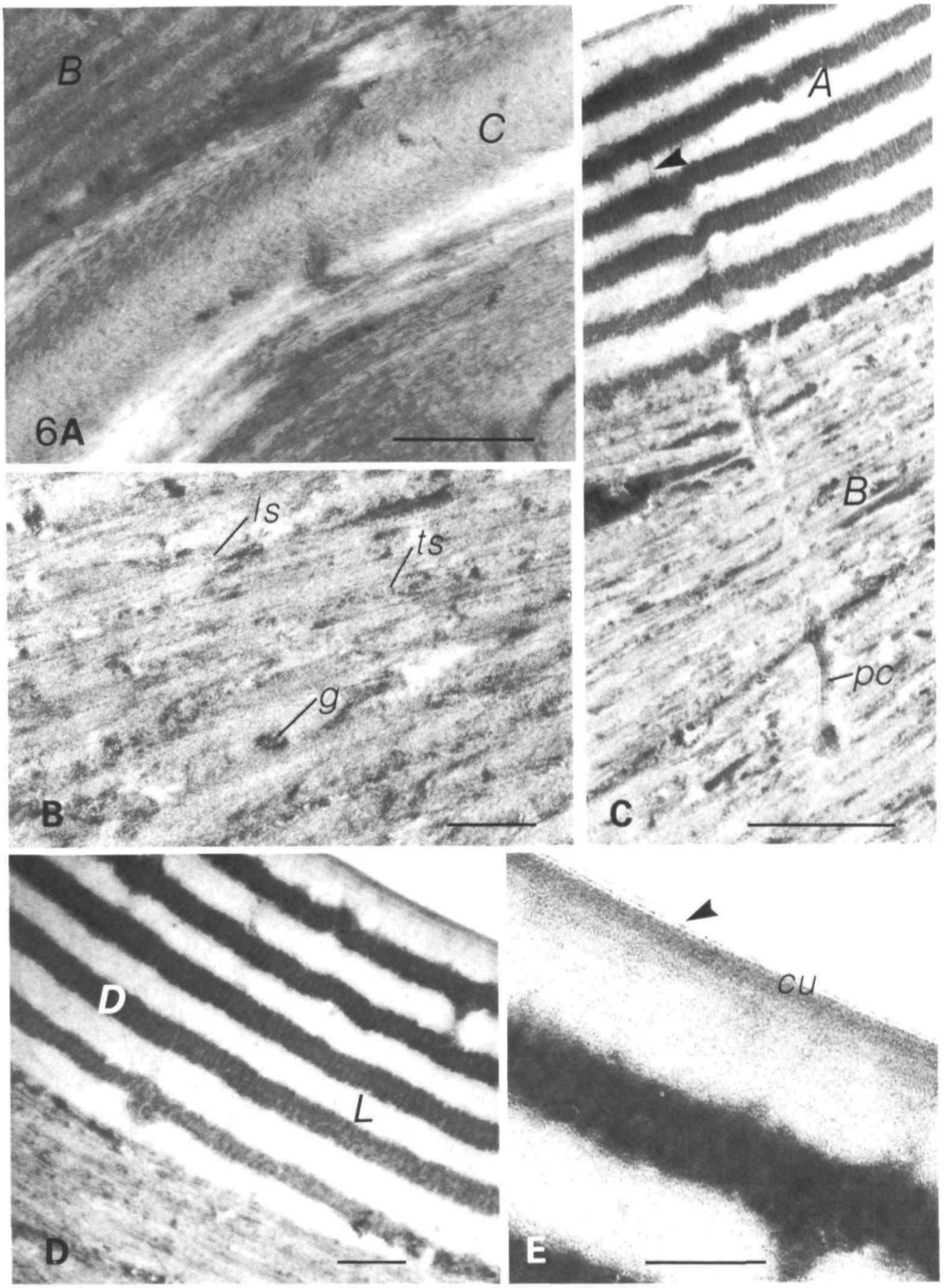

Fig. 6.

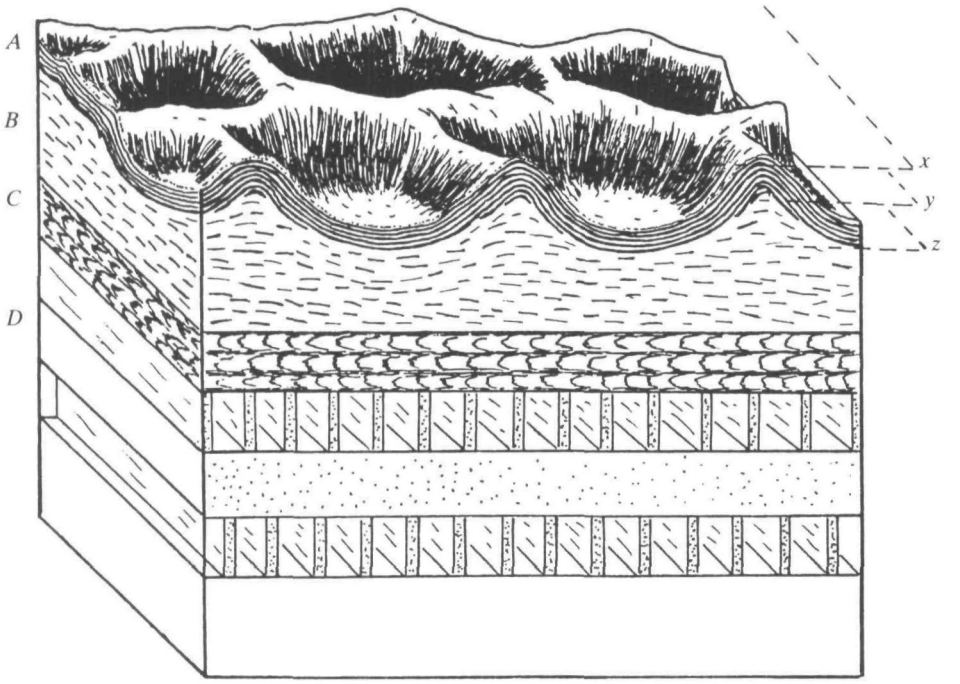

Fig. 7. Morphology and proposed terminology of the eltyral cuticle in *Cicindela*. (*D*) Endo- or mesocuticle. (*C*) Inner exocuticle. Two or three lamellae appear as a result of helicoidally oriented fibrils. (*B*) Outer exocuticle. Very fine lamellae result from the non-perfect helicoidal arrangements of fibrils. (*A*) Epicuticle. The layer assumes the outermost position and consists of alternating layers of electron-lucent and electron-dense material. No fibrillar structure is evident. Sections cut in the plane of the surface are represented by x, y and z (see text).

through the hexagonal ridges and across the intervening alveoli. Initial sections thus possess holes, surrounded by material from adjacent ridges (section x in Fig. 7). Within the ridge itself, the section passes obliquely across the outermost epicuticular layers, resulting in concentric rings around the hole. As the section intersects the ridge axis, it passes through the portion of an epicuticular layer that is oriented parallel to the section; this therefore appears as a continuous patch of either electron-dense or electron-lucent material. Deeper sections include the elevated portions of outer exocuticle within the base of a ridge (section y through region B in Fig. 7). Sections taken across the alveolar basin (section z in Fig. 7) result in a central spot of light or

Fig. 6. The ultrastructure of the outer cuticular layers in the elytron of *Cicindela formosa*. (A) Arcuate fibril pattern of layer *C* (presumptive inner exocuticle). Scale bar, 0·5 μm. (B) Fibril pattern of region *B* (presumptive outer exocuticle). Fine lamellae appear as the result of a semi-arcuate pattern of fibrils cut in longitudinal section (*ls*) and in transverse section (*ts*). Granules (*g*) of electron-dense material appear between lamellae. Scale bar, 0·2 μm. (C) Pore canal (*pc*) extending from the presumptive exocuticle (*B*) to the presumptive epicuticle (*A*). Narrow extensions of the canal are visible in layer *A* (arrow). Scale bar, 0·5 μm. (D) Ultrastructure of the presumptive epicuticle. The layer is composed of alternating layers of electron-lucent (*L*) and electron-dense (*D*) material. Scale bar, 0·2 μm. (E) High magnification of the outer edge of the presumptive epicuticle. An area of higher density in the outermost *L* layer represents the presumptive cuticulin layer (*cu*). An extremely thin (10 nm), electron-lucent layer appears between the cuticulin layer and the edge of the embedding medium (arrow). Scale bar, 0·1 μm.

dense epicuticular material ringed by obliquely sectioned layers. These islands of epicuticle are surrounded by exocuticle.

The horizontal sections demonstrate that electron-dense and electron-lucent layers have the same individual density and location when observed horizontally or vertically (Fig. 8A). The banding pattern is not, therefore, an artifact of diffraction. The layer

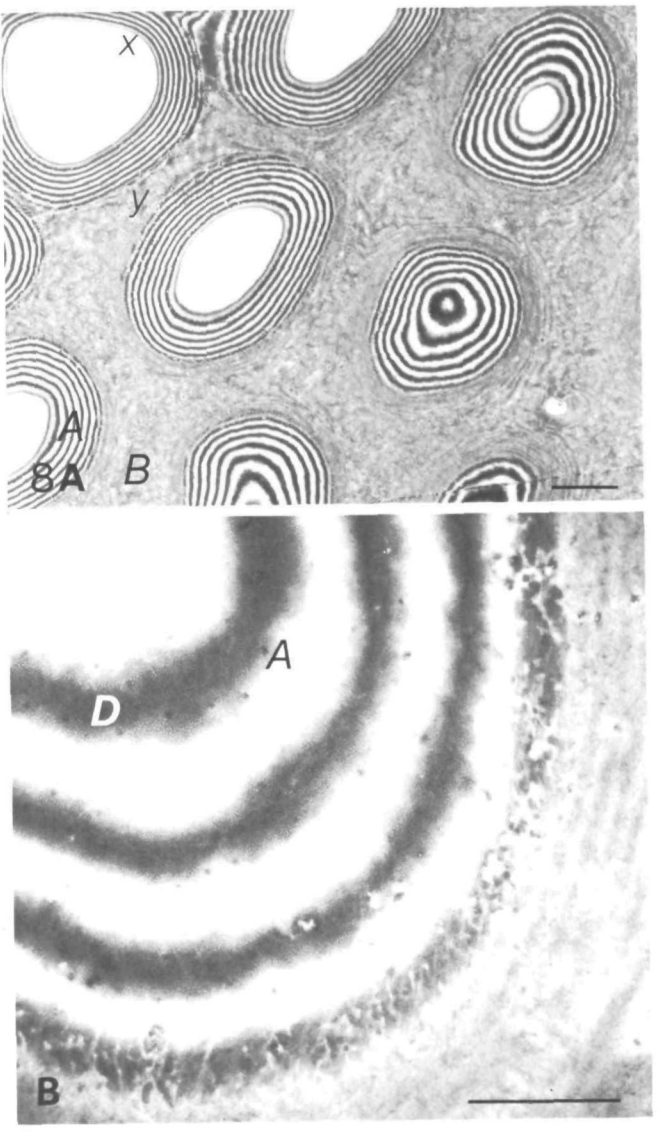

Fig. 8. (A) Transmission electron micrograph of the epicuticle (*A*) and the outer exocuticle (*B*) of *Cicindela scutellaris* sectioned in the plane of the elytral surface. Concentric rings of epicuticular material surround holes where the section did not include the basin of an alveolar cell (area *x*, see Fig. 7). The rings of epicuticle are surrounded by outer exocuticle in areas where the section includes tissues below the epicuticle within the alveolar ridges (area *y*, see Fig. 7). Note that the sequence of light and dense banding is the same as in cross-sections of the epicuticle (Fig. 5). Scale bar, 5 μm. (B) Planar section of an alveolar basin (see section *z*, Fig. 7). Note the particulate ultrastructure of the electron-dense layers (*D*) in the epicuticle (*A*). Scale bar, 1 μm.

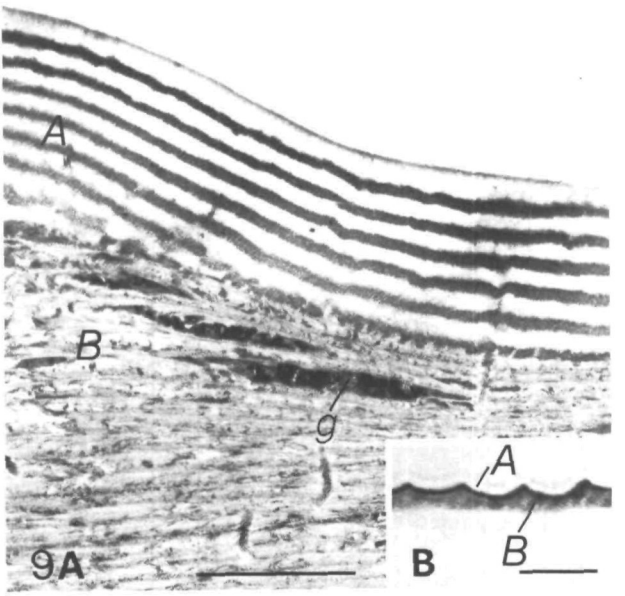

Fig. 9. (A) Transmission electron micrograph cross-section of the epicuticle (*A*) and outer exocuticle (*B*) of *Cicindela formosa*. The section was taken from a pigmented and iridescent area of the elytron. Granules (*g*) of electron-dense material appear in the exocuticle. Scale bar, 1 μm. (B) Photomicrograph of the same tissue. The epicuticle (*A*) and exocuticle (*B*) are pigmented and highly refractive. Scale bar, 10 μm.

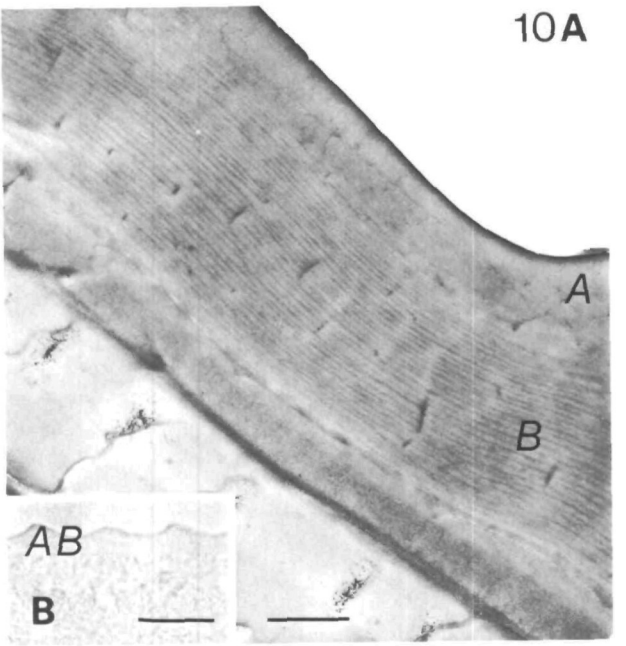

Fig. 10. (A) Transmission electron micrograph of a cross-section of elytral cuticle sectioned from the non-pigmented maculations of *Cicindela formosa*. Electron-dense layers are absent from the epicuticle (*A*). Scale bar, 1 μm. (B) Photomicrograph of the same non-pigmented tissue. The epicuticle and outer exocuticle (*AB*) show no pigmentation or higher refractivity than the underlying cuticle. Scale bar, 10 μm.

that borders the holes in horizontal sections is the outermost layer of the epicuticle, and is electron-lucent in both orientations. Furthermore, horizontal sections within a single epicuticular layer show continuous patches of electron-dense material. This material is very finely particulate when viewed perpendicular to the layer (Fig. 8B).

When thin sections are viewed through an optical microscope, the outer exocuticle and the epicuticle appear dark brown (Fig. 9B). This apparent pigmentation is confined to the outer 5 μm of the elytral cuticle. It is assumed that the dark brown appearance is due to the presence of melanin in this region, and that it is responsible for the dark opaque appearance of the elytron in transmitted light. The epicuticle and outer exocuticle display a greater retardation of light than the inner layers of procuticle under interference microscopy.

Sections of elytral cuticle were also cut from the white maculations of *C. formosa*. The white areas show no trace of either iridescent colour or brown or black pigmentation (Fig. 10B). Under interference microscopy, the sections of white cuticle show a uniformity in refractive index throughout the elytron. The epicuticle shows a refractive index of approximately 1·5 by the Becke line test (Neville, 1980).

Electron micrographs of this non-pigmented cuticle show an epicuticle which lacks the electron-dense bands (layer *A* in Fig. 10A). In general, this homogeneous epicuticle is thinner and lower in contrast than the laminated epicuticle of pigmented areas (layer *A* in Fig. 9A). SEM confirmed the absence of the epicuticular laminations in the region of the elytral maculations. The outer exocuticle of these sections lacks the electron-dense granules that were evident in the exocuticle of pigmented areas (layers *B* in Figs 9A and 10A).

Analysis of cuticle structure by chemical treatment

Tiger beetle cuticle treated with dilute KOH displayed a gradual loss of structural coloration, as well as pigmentation. Immersion in ethanol, xylene, acetone, sulphuric or nitric acid failed to produce any change in structural colour. Initially, structural colours became longer in wavelength as the solvent temporarily swelled the reflectance layers. After 4 h, however, the maroon portion of the elytron of *C. formosa* appeared blue-green. The anterior portion, originally red, became ochreous with slight orange-green reflections. The overall iridescence was reduced to a dull sheen. Scanning electron micrographs of the treated elytra revealed a distorted and heavily eroded surface microsculpture. Under transmission electron microscopy, the regular laminations at the periphery of the cuticle were disrupted and often stripped from the sample (Fig. 11).

With the exception of a few blue-green or violet reflections in the basins of punctures, elytra treated with KOH for 12–15 h were virtually devoid of structural colours. The surface had a flat, brown, darker appearance at the elytral base, which is assumed to be due to the residual presence of melanin in the exocuticle. The deep hexagonal depressions of the surface microsculpture were eroded to a shallow outline of the surface pattern. TEM micrographs revealed that the laminated epicuticle was completely removed from the surface of the outer exocuticle (Fig. 12). A light band, 0·29 μm thick, remained at the border of the exocuticle. The exocuticular lamination also became more obscure and fragmented.

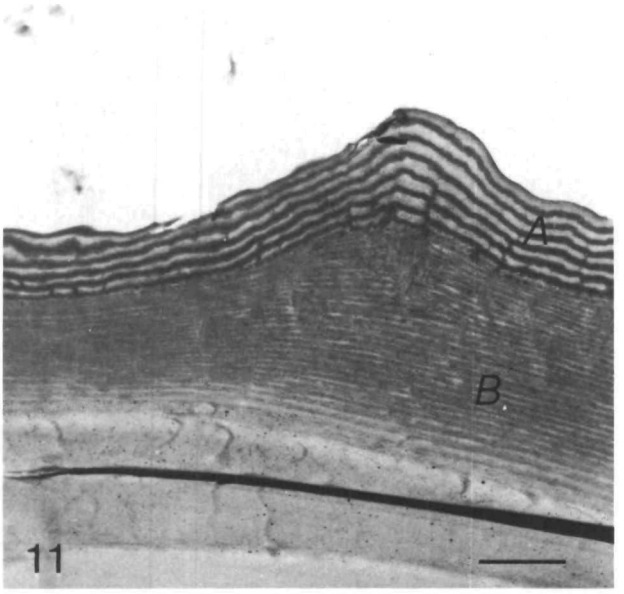

Fig. 11. Transmission electron micrograph of a cross-section of elytral cuticle of *Cicindela formosa* treated for 4 h with 8% KOH. The epicuticular layers are disrupted and partially dispersed. (*A*) epicuticle, (*B*) outer exocuticle. Scale bar, 1 μm.

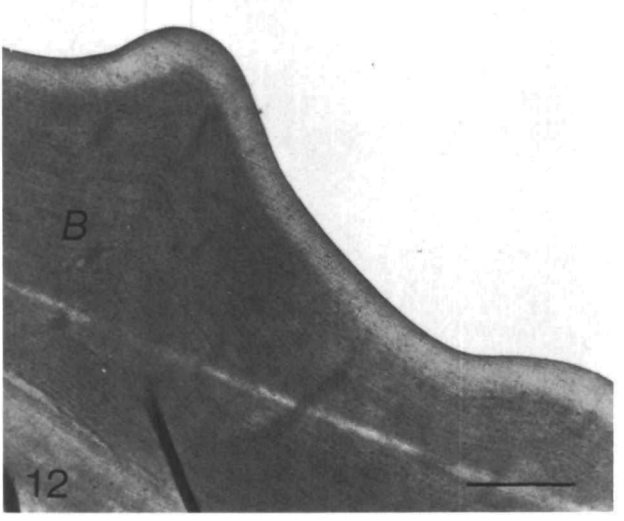

Fig. 12. Transmission electron micrograph cross-section of elytral cuticle of *Cicindela formosa* treated for 15 h with 8% KOH. The epicuticle is dissolved completely. An area of lower electron density appears near the exposed surface of the outer exocuticle (*B*). Scale bar, 1 μm.

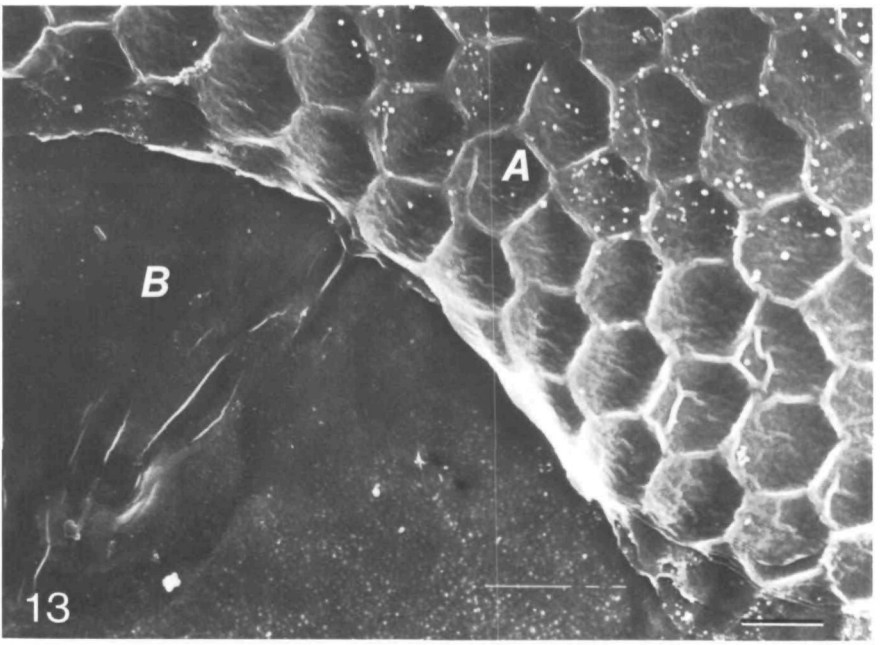

Fig. 13. Scanning electron microscope surface view of an elytron of *Cicindela scutellaris* treated for 15 min with concentrated KOH at 160 °C. In area *A*, the epicuticle is intact, but eroded. This area was still weakly iridescent. In area *B*, the epicuticle has been removed, exposing the surfaces of the exocuticle. This surface was non-iridescent. Scale bar, 10 μm.

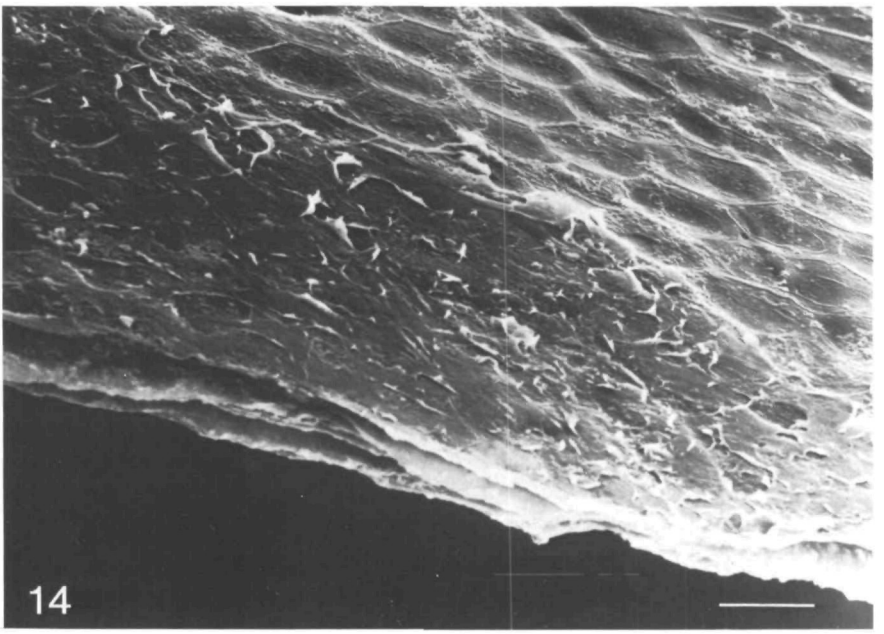

Fig. 14. Scanning electron microscope surface view of an elytron of *Cicindela formosa* treated for 15 min with concentrated KOH at 106 °C. The epicuticle has been dissolved. This sample was no longer iridescent. Scale bar, 10 μm.

Longer KOH treatments resulted in a progressive loss of the remaining brown colour. By 48 h, only a slight trace of the original maculation pattern was evident, and the elytron was a light straw colour. During this treatment, the outer exocuticle remained – the alveolate pattern was still visible in the surface. However, the thickness of this layer was reduced by 40 %, suggesting a leaching of exocuticular components.

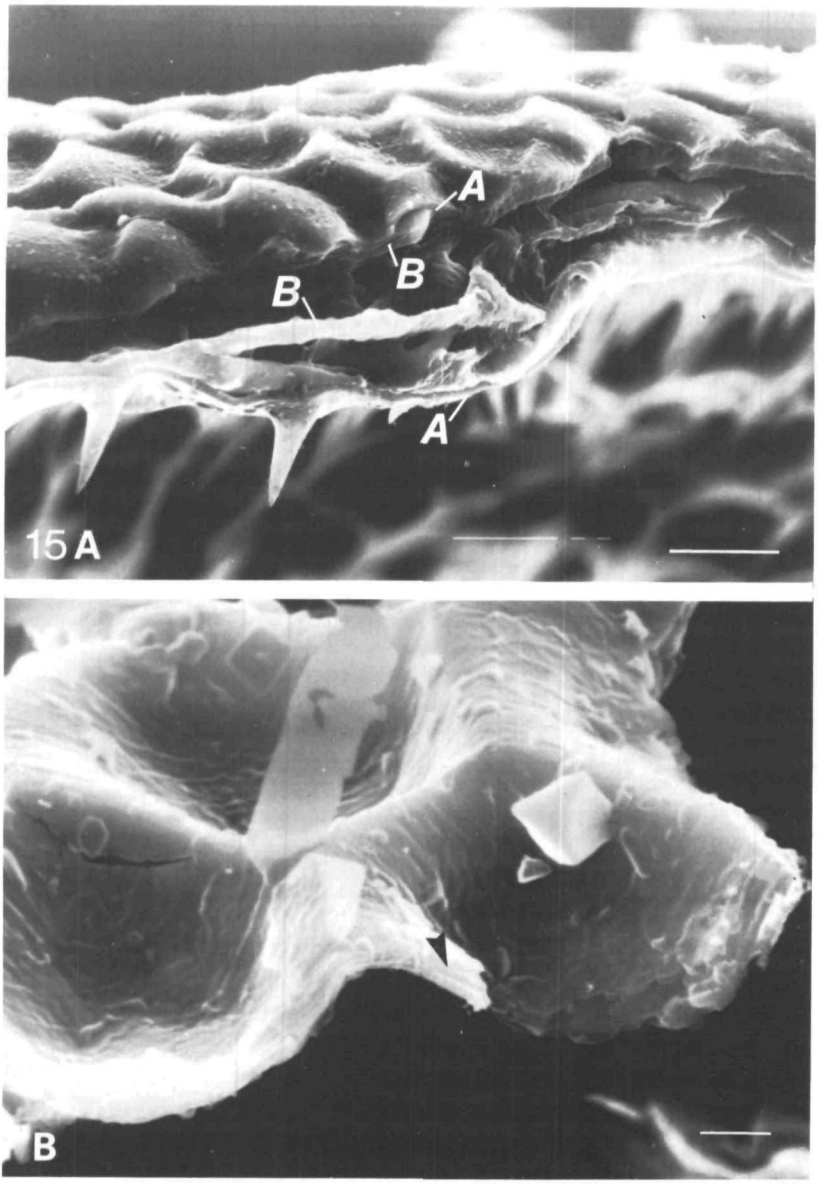

Fig. 15. Scanning electron microscope cross-section of an elytron of *Cicindela formosa* treated with concentrated H_2SO_4 for 48 h. (A) The endocuticle of the elytron has been dissolved, leaving a sleeve of epicuticle (*A*) and exocuticle (*B*). Scale bar, 10 μm. (B) A portion of the epicuticle separated from the outer exocuticle. Surface pattern and laminations are still intact (arrow). Scale bar, 2 μm.

The chitosan method of Campbell (1929) and van Wisselingh (1914) has long been used to distinguish chitinous from non-chitinous cuticle, although this technique is not conclusive (Richards, 1951). It requires the conversion of chitin to chitosan by treatment with concentrated KOH at 160 °C for 15 min. It is assumed that the non-chitinous elements of the exoskeleton (epicuticular components) are dissolved under

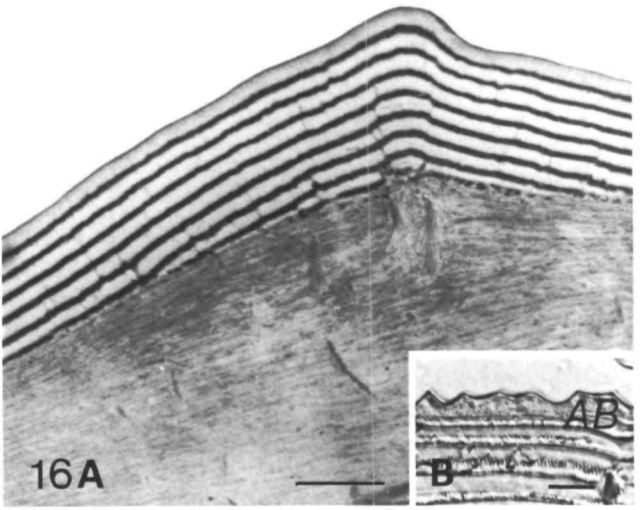

Fig. 16. (A) Transmission electron microscope cross-section of pigmented cuticle of *Cicindela formosa* treated with H_2O_2. The electron-dense layers of the epicuticle are reduced in thickness (compare with Fig. 9). Outer layers appear most reduced by the treatment. Scale bar, 1 μm. (B) Photomicrograph of the same tissue. The epicuticle and exocuticle (*AB*) are not strongly pigmented. Scale bar, 10μm.

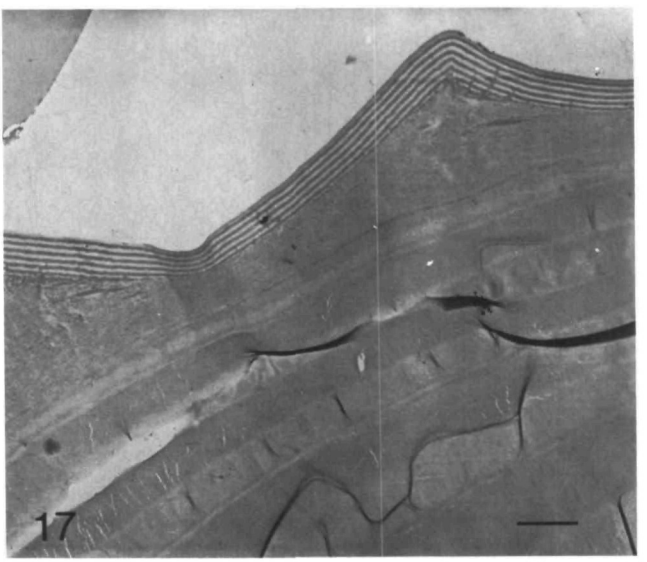

Fig. 17. Transmission electron micrograph cross-section of the elytral cuticle of *Cicindela repanda*. The epicuticle (*A*) is laminated, although no peak interference colour is reflected. Scale bar, 2 μm.

this alkali treatment. Samples of tiger beetle cuticle subjected to the chitosan test showed a severe break-up of the presumptive epicuticle. In *C. scutellaris*, an eroded epicuticle (area *A* in Fig. 13) was evident in some areas where a feebly iridescent sheen still appeared. If these treated samples were immersed in 8 % KOH for 18 h at room temperature, all traces of the presumptive epicuticle were removed, as well as the remaining pigmentation. In *C. formosa*, the epicuticle and iridescence were completely removed by the chitosan treatment (Fig. 14).

In contrast to the results of the alkali treatments, endocuticle is dissolved rapidly in concentrated sulphuric acid (Sprung, 1931; Wigglesworth, 1933; Hackman, 1974), whereas sclerotized exocuticle and epicuticle are said to remain intact. Tiger beetle elytra immersed in sulphuric acid showed a rapid dissolution of inner 'plywood' mesocuticle, leaving a thin, flexible sleeve of putative epicuticle and outer exocuticle, while the structural coloration of the elytron remained unaltered (Fig. 15A). SEM examinations of the treated cuticle revealed that the outer laminated layer (layer *A*) retained its ultrastructure intact (Fig. 15B). The outer exocuticle was also intact and pigmented through the first 48 h of treatment. The residual cuticle still appeared dark brown in transmitted light. Portions of the helicoidal exocuticle below could be seen adhering to the lower side of the outer exocuticle. Frequently, areas were observed in which the epicuticle had separated from the outer exocuticle, and these fragments were found floating on the surface of the acid. Even these isolated fragments maintained a laminated appearance under SEM, as well as an iridescence.

Treatments of elytral cuticle with H_2O_2 significantly altered the cuticle coloration. When observed in transmitted light, the brown coloration became more translucent. The outer exocuticle and epicuticle appeared either light brown or clear of pigment in microscopic sections (Fig. 16B). The structural colour of the cuticle surface became duller and shorter in principal wavelength. Similar results were obtained when samples were treated with 20 % H_2O_2 at 26 °C for 24–48 h.

TEM micrographs revealed a 40 % reduction in thickness of dense epicuticular layers in the H_2O_2-treated samples (Fig. 16A). The bands were progressively thinner towards the outer surface. The overall thickness of the epicuticle was not diminished significantly.

DISCUSSION

Cuticle histology

Probably because it is extremely thin, the epicuticle is the least understood portion of the insect integument. Its chemistry, structure and the terminology of epicuticular components have been controversial. Only a few, diverse arthropods have been studied intensively, and very little work has focused on the epicuticle of hard, adult exoskeletons (Delachambre, 1970). This is not surprising since hard cuticle is difficult to prepare and section for transmission electron microscopy.

The epicuticle, by definition, is non-chitinous or reacts negatively to tests for chitin (chitosan method). It is the first layer formed during the moult sequence and assumes the outermost position in the strata of the exoskeleton, bearing the surface microsculpture. The general model of epicuticle structure recognizes five components. These are the cuticulin layer, the inner epicuticle, the outer epicuticle, the wax layer

and the cement layer, listed in order of deposition (Filshie, 1982). The wax and cement layers are secreted upon the epicuticular surface by the epicuticular filaments and dermal glands, respectively. Filshie (1982) notes that the saturated lipids of wax layers do not survive conventional electron microscope preparations, and their supposed appearance in electron micrographs is probably an artifact or misidentification of other layers. Identifications of cement layers have been made by location only and remain unsupported by developmental studies.

The reflective layers of cicindelid cuticle are not a form of cement or tectocuticle. The so-called 'Sekretschicht'–the source of the structural colours–is formed preecdysially, not secreted from dermal glands (Schultz & Rankin, 1985). Furthermore, the very even pattern of layering over a contoured surface would be unlikely if it were formed from secretions of relatively dispersed glands. The layers remain evenly spaced around and even within the mouth of dermal glands (Fig. 4). Extraordinary properties of the two components and the dermal glands themselves would be required to produce such regular secretions over the entire cuticular surface.

The cuticulin layer (or outer epicuticle of Neville, 1975) is the first epicuticlar layer secreted by the epidermis during the moult sequence. It appears as a thin (10–20 nm), dense membrane at the outer edge of the cuticle in electron micrographs. In some insects (Locke, 1966; Delachambre, 1970), it initially appears laminated, but condenses to a uniform appearance. Micrographs of *C. formosa* show a dense region, 30–40 nm thick, at the edge of the outermost electron-lucent band (*cu* in Fig. 6E). The inner side of this region appears finely laminated, becoming more uniformly dense towards the surface of the cuticle. This region appears in all the *Cicindela* species and samples studied, including the pharate cuticle (see Schultz & Rankin, 1985), and is interpreted as the cuticulin layer. In mature cicindelid cuticle only, a very thin (10 nm), electron-lucent membrane appears above the cuticulin. This structure may represent the outer epicuticle that is thought to arise by separation from the cuticulin layer prior to ecdysis (Filshie, 1982).

The bulk of the epicuticle is composed of the inner epicuticle, 0·5–1 μm thick. Its appearance varies among species, and consequently, a wide range of chemical constituents have been proposed. These include protein, lipids, lipoprotein and dihydroxyphenols. This layer borders directly on the helicoidal exocuticle beneath it (Neville, 1975). Laminated inner epicuticles have been described, but these laminations have been transitory during the moult sequence (Delachambre, 1970), or have extremely short periods of less than 40 nm (Gupta & Smith, 1969; Gluud, 1968; Zacharuk, 1972).

The multilayered outer region of cicindelid cuticle is best described as inner epicuticle, due to its location, ultrastructure and solubility in KOH, in combination with a resistance to strong acid (Region *A* in Figs 2–7). Treatments with solvents demonstrate that this region is chemically distinct from the chitinous layers below. If it were exocuticle, the ultrastructure of the layers would survive the alkali treatment (Hackman, 1974). Furthermore, it lacks any indication of fibrillar architecture that is evident in the alkali-resistant layers or in the exocuticles of other insects.

The outermost layer of inner epicuticle, presumably secreted first, is always electron-lucent, while the innermost layer may be electron-lucent or electron-dense. More layers are produced at the borders of the epidermal cells than at their centres.

These borders are indicated by the hexagonal ridges in the surface microsculpture (Neville, 1975). Areas of elytral cuticle which lack pigmentation (i.e. the maculations), also lack electron-dense layers in the epicuticle. Perhaps the cicindelid inner epicuticle is described best as a homogeneous electron-lucent material, impregnated by electron-dense material at discrete intervals in those cuticles that are pigmented.

The epicuticle as an interference reflector

It appears that the epicuticle is the source of structural colours in *Cicindela*. Maceration or removal of the epicuticle with KOH results in the deterioration or loss of iridescent coloration. Conversely, removal of the other components of the integument produces no loss of colour. The change of hue under oblique incidence demonstrates that the structural colours result from constructive interference of reflected light.

The repetitive layering of two materials in the epicuticle, whose thicknesses are less than half the wavelength of visible light, is characteristic of a multilayer interference reflector. The two layers are distinct in their electron densities, and are not an artifact of the helicoidal arrangement of cuticle fibrils, as in the reflective exocuticle of optically active scarab beetles (Neville & Caveney, 1969). Multilayer reflectors have been described in a wide diversity of animal tissues, and the basic principles of interference in animal reflectors are reviewed by Land (1972).

In the 'ideal' case of thin film reflection, the wavelength of the first order maximum reflectance (λ max) depends on the thickness (d) and refractive index (n) of each layer such that

$$\lambda \max = 4nd \sin \theta, \tag{1}$$

where θ is the angle of incidence. Under 'ideal' conditions, the optical thicknesses of both layers are equivalent ($n_L d_L = n_D d_D$, where L indicates the lucent layer and D the dense layer). Each layer acts as a quarter-wavelength reflecting plane, with the reflections from all interfaces constructively interfering to produce the total coloration.

The optical thickness of each component is different ($n_L d_L \neq n_D d_D$) in a 'non-ideal' multilayer system. The first order reflectance peak occurs at

$$\lambda \max = 2(n_L d_L + n_D d_D) \tag{2}$$

under normal angle of incidence. Under 'non-ideal' conditions the peak reflectance and the band width of the first order peak are diminished. The result is a sharper peak and purer colour (Land, 1972). The reflecting layers of tiger beetle epicuticle are best described as a 'non-ideal' system. The thicknesses of the electron-dense (d_D) and the electron-lucent (d_L) layers vary considerably through a single point in the stack (Table 1). Assuming that the refractive indices (n_L and n_D) remain stable, the ratio d_L/d_D does not remain constant throughout the reflector.

A quarter-wave interference reflector has been described by Durrer & Villiger (1972) in the exocuticle of *Euchroma gigantea*, which consists of a series of electron-lucent and electron-dense bands similar to the epicuticle of *Cicindela*. The dimensions of the layers imply an average refractive index of 1·75 for the reflector. The authors propose that the multilayer system contains electron-dense melanin layers (RI = 2·0) separated by chitin (RI = 1·5), similar to the keratin-melanin interference

Table 1. *Average thickness of electron-lucent* (L) *and electron-dense* (D) *layers in four* Cicindela *species with predicted and experimental values of elytral reflectance*

Specimen	SEM bilayer thickness (nm)	Mean L layer thickness (nm)	Mean D layer thickness (nm)	Calculated λ max (nm) $n_L = 1{\cdot}5$; $n_D = 2{\cdot}0$	Experimental λ max (nm)
C. formosa					
ridge	188	106·59 ± 6.76	93·63 ± 11·756	694·31	655
alveolar basin		101·99 ± 5·292	74·974 ± 6·752	605·77	
C. scutellaris rugata	143	67·197 ± 4·08	72·147 ± 4·591	489·93	499
C. splendida	178	102·03 ± 14·907*	71·428 ± 6·563	591·8	635
C. repanda					
ridge	—	137·73 ± 18·233	110·65 ± 12·156	855·79	—
alveolar basin		81·22	88·035 ± 6·815	595·8	

Standard deviation values indicate the variation between successive layers in the epicuticle.
Calculations of λ max assume a refractive index (n) of 1·5 for L layers and 2·0 for D layers.
* The outermost L layer measured 130 nm in this sample.

reflectors of bird feathers (Durrer & Villiger, 1970). In their approach, the authors calculated the wavelength of maximum reflectance for each layer separately, in addition to determining the reflectance from the series of bilayers (equation 2). They concluded that a mixture of these reflected components results, producing the total colour.

Mossakowski (1980) examined interference reflectors in the cuticles of the buprestid, *Chrysocroa vittata*, and the tiger beetle, *Cicindela campestris*. Mossakowski calculated reflectances for a number of possible refractive indices using the theoretical treatment of Huxley (1968). He proposed that an average refractive index of 1·75 for the bilayers of *C. camprestis* would cause a total reflectance value far exceeding those determined experimentally. Mossakowski's measurements of total reflectance predicted refractive indices of 1·5 and 1·6 for the light and dense layers respectively. However, these values and the dimensions of the layers observed under electron microscopy predicted a wavelength of peak reflectance substantially below those recorded spectrophotometrically. Mossakowski assumed that the reflecting layers had experienced a 10–15 % shrinkage due to specimen preparation or exposure to the electron beam.

The dimensions of the interference layers of cicindelids presented in this paper suggest a relatively high average refractive index near 1·75 for the pairs of layers. Values of 1·5 and 2·0 for the light and dense layers predict peak wavelengths which approximate to the spectrophotometric results for *C. scutellaris* and *C. formosa* (Table 1). Refractive indices of 1·5 and 1·6 would predict substantially shorter wavelengths of peak reflectance. The epicuticle of *C. repanda* varied greatly in layer thickness and its reflectance exhibited no single peak within the visible wavelengths.

Even assuming an average refractive index of 1·75, calculations using the average thicknesses of epicuticular layers predict values of λ max well below the reflectance peak of *C. splendida*. Unlike the other specimens, the outermost electron-lucent layer of *C. splendida* is 40–50 nm thicker than all the underlying electron-lucent layers.

This layer makes a significant contribution to the large standard deviation in the average thickness of these layers. Variation in the thickness of the inner layers is less than that of *C. repanda* but greater than the variation in *C. scutellaris*. A λ max of 638 nm is predicted if calculations are based upon the superficial electron-lucent layer ($d_L = 130$ nm, $n_L = 1{\cdot}5$) and the underlying dense layer ($d_L = 62$ nm, $n_L = 2{\cdot}0$). This value is close to the experimental reflectance peak of 635 nm. Since the surface of *C. splendida* is so deeply sculptured with the alveolate pattern, the superficial epicuticular layers may contribute more to the peak reflectance than the underlying layers. Peak reflectances from deeper layers may occur at angles which depart from the angle of reflection that is sampled by the spectrophotometer.

In *C. scutellaris rugata* and the green form of *C. campestris* (Mossakowski, 1980), the thickness of the light and dense layers are roughly equivalent. In these cases, the average refractive index $\bar{n}$ may be estimated from the experimental peak wavelength and the thickness of each bilayer (d_{DL}):

$$\lambda \max = 2\bar{n}d_{DL} \tag{3}$$

$$\text{or } \bar{n} = \lambda \max/2d_{DL}. \tag{4}$$

For *C. scutellaris rugata*, an average refractive index of 1·74 is predicted.

No evidence of shrinkage appeared in the samples of cicindelid cuticle. The structural colours of specimens were observed unchanged within the embedding medium, indicating that shrinkage did not result from specimen preparation. SEM measurements of epicuticular bilayers corresponded well with bilayer measurements made from transmission electron micrographs. If bilayers measured from SEM micrographs were assumed to shrink 10% under the electron beam, they would appear 10–20 nm thinner than the average thickness of bilayers measured from TEM micrographs. If shrinkage had occurred under the electron beam, TEM measurements should fall below the thicknesses measured under SEM.

The relatively low total reflectance of cicindelid epicuticle may be due to its alveolate microsculpture. If the angle of incident light departs from normal, the wavelength of peak reflectance becomes shorter according to

$$\lambda \max = 4nd \cos \theta, \tag{5}$$

where θ is the angle of refraction within a single layer. In addition, each successive epicuticular layer conforms to the alveolate pattern of the surface. The wavelength of peak reflectance for multilayer reflectors at oblique incidence is then given by:

$$\lambda \max = 2(n_L d_L \cos \theta_L + n_D d_D \cos \theta_D), \tag{6}$$

where θ is the angle of incidence in the layer of lower density. Similarly, the reflectance at each interface is dependent upon the angle of refraction (Land, 1972). Thus, the wavelength and the intensity of reflection are affected by deviations in angle of incidence and refraction which occur continuously throughout the horizontal dimensions of the epicuticular layers. Due to these effects, and the scattering of reflected light by an alveolate surface, the spectrophotometric analysis of reflected light from the epicuticle must surely underestimate the reflectance predicted by normal theoretical conditions.

The peak reflectance is also dependent upon the constancy of layer thickness throughout the epicuticle. In *Cicindela*, the thicknesses of the bilayers vary both horizontally and vertically within the epicuticle (Table 1). The theoretical treatment of non-ideal, multilayer reflectors assumes that these dimensions remain constant. This non-uniformity in layer thickness and angle, with respect to incident light, clearly places the cicindelid epicuticle as an extremely complex example of a biological interference reflector. The epicuticle represents a non-ideal, multilayer system moulded into a shallow honeycomb form, and is not adequately described by theoretical treatments for regularly spaced, planar systems.

Correlations between electron microscope measurements and reflectance data should not be over-emphasized. The amount of cuticle sectioned is not comparable to the area of elytral material sampled for reflectance. The variability within the interference reflector has already been described. In addition, there is always uncertainty as to whether the section is precisely perpendicular to the interference layers.

With rare exceptions, the brown or black colours of insect cuticles are attributed to sclerotization and/or melanization of the cuticle (Richards, 1967). Eumelanins predominate as the brown or black pigments of insect integument (Hackman, 1974), and the pigmentation of *Cicindela* has been ascribed to melanin since the work of Shelford (1917). Unfortunately, it is exceedingly difficult to identify small amounts of melanin by staining or chemical analysis. Since the individual layers of dense material in the epicuticle are not resolvable under light microscopy, their optical properties cannot be examined separately. The treatment with KOH removes the epicuticle from the pigmented exocuticle, and produces a solution that is stained brown with dissolved epicuticle. But it is also possible that melanin may be leached from the exocuticle by the treatment (Richards, 1967).

Richards (1967) found that treatment with H_2O_2 will bleach melanin particles without removing them from the cuticle. Tiger beetle elytra were treated with H_2O_2 to determine the role of melanin in the elytral coloration. If melanin is involved simply as an absorbent background to the interference reflector, the iridescent colour should be reduced in intensity, but not altered in hue when the pigment is bleached (Mason, 1927). In treatments of *C. formosa*, a reduction in intensity and predominant wavelength resulted, as well as a thinning of pigmented colour in the cuticle. The change in reflected colour may be due to the bleaching of melanin within the structure of the reflecting epicuticle itself.

The structural dimensions of the two epicuticular layers, in conjunction with the experimental reflectance results, suggest that the epicuticular reflector is composed of an electron-lucent layer with a refractive index of 1·5 and a dense layer of 2·0. A refractive index of 1·5 is acceptable for insect cuticular proteins (Neville, 1975). This study proposes that the unusually high refractive index of 2·0 is provided by layers of melanin or melanoproteins. Precedents for such a system can be found in iridescent bird feather colouration (Greenwalt, Brandt & Friel, 1960; Rutschke, 1966; Durrer & Villiger, 1966, 1970). Additional melanin in the outer exocuticle provides an absorbent background for transmitted and extraneous wavelengths, hence purifying the reflected colour. Circumstantial evidence for the role of melanins is found in the restrictive co-occurence of pigmentation, iridescence and epicuticular lamination. Specific chemical analysis is still required to verify the identity of the electron-dense layer as melanin.

Structural coloration in Cicindela

The specific coloration of structurally-coloured tiger beetles depends upon the relative thicknesses of the epicuticular layers. In *C. formosa, C. scutellaris* and *C. splendida*, the dimensions of these layers are sufficient to cause the constructive interference of visible wavelengths of light. In epicuticles with regular laminations and a relatively smooth microsculpture, as in *C. scutellaris*, the reflectance colours are purer.

In some areas of *C. repanda* elytra, epicuticular laminations are too wide to reflect light at visible wavelengths (Fig. 17). However, visible wavelengths are reflected from areas where the layers are sufficiently thin in the highly variable epicuticle, e.g. within the alveoli. Furthermore, visible wavelengths may be reflected from thicker layers at oblique incidence due to the effect of angle of incidence on the wavelength of maximum reflectance. Thus, while the layers of *C. repanda* may reflect maximally above 760 nm, shorter red wavelengths will be reflected by the highly angled pattern of ridges in the microsculpture. The results of these factors is a relatively poor reflectance of any one visible wavelength, producing an overall flat brown appearance upon casual observation. Under the dissecting microscope, a wide range of reflected colours (predominantly red) can be observed from various points on the surface microsculpture. Although at first glance the elytra of *C. repanda* do not appear to be structurally coloured, the epicuticular structure is consistent with the epicuticular reflectors of other iridescent species.

Thus, tiger beetle structural coloration depends upon three variables: the thickness, uniformity and microsculpture of the reflecting layers. In species which reflect a narrow band of short wavelengths, the epicuticular bilayers are relatively thin and the intensity and purity of the colour depend upon the severity of the alveolate microsculpture. Several species which appear brown or coppery bear relatively thick and variable epicuticular bilayers. The deeply pitted microsculpture of the reflector further diminishes the intensity and purity of the reflected colour, resulting in a broad range of reflected wavelengths of low intensity. Small variations in the basic multilayer structure of the epicuticle are responsible for the wide variation in colour observed in the genus *Cicindela*.

The authors thank Dr S. Meier, University of Texas, for the use of the SEM, Dr Bird and K. Kotora of Rutgers University, for their assistance in the reflectance spectrophotometry, and the Texas Department of Parks and Wildlife for permission to collect specimens. We especially appreciate the assistance of Susan Houghton, MBL, Woods Hole, MA, who sectioned and photographed the TEM material. This study was supported partially by NSF Grant 2610711250.

REFERENCES

Bernard, G. D. & Miller, W. H. (1968). Interference filters in the corneas of Diptera. *Invest. Ophthamol.* **7**, 416–434.

Biedermann, W. (1914). Farbe und Zeichnung der Insecten. In *Handbuch Vergleichende Physiologie*, (ed. H. Winterstein), pp. 1657–1994.

Bouligand, Y. (1972). Twisted fibrous arrangements in biological materials and cholesteric mesophases. *Tissue Cell.* **4**, 189–217.

CAMPBELL, F. L. (1929). The detection and estimation of insect chitin; the irrelation of chitinization to hardness and pigmentation of the cuticula of the American cockroach, *Periplaneta americana*. *Ann. ent. Soc. Am.* **22**, 401–426.

DELACHAMBRE, J. (1970). Etudes sur l'épicuticle des insectes. La développement de l'épicuticle chez l'adulte de *Tenebrio molitor* L. (Insecta: Coleoptera). *Z. Zellforsch. mikrosk. Anat.* **108**, 380–396.

DURRER, H. & VILLIGER, W. (1966). Schillerfarben der Trogoniden. *J. Orn., Lpz* **107**, 1–36.

DURRER, H. & VILLIGER, W. (1970). Schillerfarben des Goldcuckucks, *Chysococcyx cupreous* Shaw, im Elektronenmikroskop. *Z. Zellforsch. mikrosk. Anat.* **109**, 407–413.

DURRER, H. & VILLIGER, W. (1972). Schillerfarben von *Euchroma gigantea* L., elektronenmikroskopische Untersuchung der Elytren. *Int. J. Insect. Morph. Embryol.* **1**, 233–240.

FILSHIE, B. (1982). Fine structure of the cuticle of insects and other arthropods. In *Insect Ultrastructure*, Vol. 1, (eds R. C. King & M. Akai), pp. 281–312. New York: Plenum Press.

GAUMER, G. C. (1977). The variation and taxonomy of *Cicindela formosa* Say (Coleoptera: Cicindelidae). Ph.D. thesis, Texas A & M University. 253 pp.

GHIRADELLA, H., ANESHANSLEY, D., EISNER, T., SILBERGLIED, R. E. & HINTON, H. E. (1972). UV reflection of male butterfly: interference colour caused by thin-layer elaboration of wing scales. *Science, N.Y.* **178**, 1214–1217.

GLUUD, A. (1968). Zur Feinstruktur der Insektencuticula. Ein Beitrag zur Frage des Eigengiftschutzes der Wanzencuticula. *Zool. Jb. (Anat.)* **85**, 191–227.

GREENWALT, C. H., BRANDT, W. & FRIEL, D. (1960). The iridescent colors of hummingbird feathers. *Proc. Am. Phil. Soc.* **104**, 249–253.

GUPTA, B. L. & SMITH, D. S. (1969). Fine structure organization of the spermatheca in the cockroach, *Periplaneta americana*. *Tissue Cell* **1**, 289–324.

HACKMAN, R. H. (1974). Chemistry of insect cuticle. In *The Physiology of Insecta*, Vol. 6, (ed. M. Rockstein), pp. 216–270. New York: Academic Press.

HASS, W. (1916). Ueber Metallfarben bei Buprestiden. *Sber. Ges. natur. Freunde Berl.* 332–343.

HEPBURN, H. R. (1972). Some mechanical properties of crossed fibrillar chitin. *J. Insect Physiol.* **18**, 815–820.

HUXLEY, A. F. (1968). A theoretical treatment of the reflexion of light by multilayer structures. *J. exp. Biol.* **48**, 227–245.

LAND, M. F. (1972). The physics and biology of animal reflectors. *Prog. Biophys. molec. Biol* **24**, 75–106.

LOCKE, M. (1966). The structure and formation of the cuticulin layer in the epicuticle of an insect, *Calpodes ethlius* (Lepidoptera: Hesperiidae). *J. Morph.* **118**, 461–494.

MANDL, K. (1931). Künstliche Veränderung der Farben an *Cicindela nitida* Licht und an anderen *Cicindela*-Arten. *Z. Morph. Okol. Tiere* **22**, 110.

MASON, C. W. (1927). Structural colors in insects. *J. phys. Chem.* **31**, 321–354.

MOSSAKOWSKI, D. (1980). Reflection measurements used in the analysis of structral colours of beetles. *J. Microscopy* **116**, 350–364.

NEVILLE, A. C. (1975). *Biology of the Arthropod Cuticle*. Berlin: Springer-Verlag.

NEVILLE, A. C. (1980). Optical methods in cuticle research. In *Cuticle Techniques in Arthropods*, (ed. T. A. Miller), pp. 45–89. New York: Springer-Verlag.

NEVILLE, A. C. & CAVENEY, S. (1969). Scarabeidae exocuticle as an optical analogue of cholesteric liquid crystals. *Biol. Rev.* **44**, 531–562.

ONSLOW, H. (1920). The iridescent colours of insects. 1. The colours of thin films. *Nature, Lond.* **106**, 149–152.

RICHARDS, A. G. (1951). *The Integument of Arthropods*. St. Paul: University of Minnesota Press.

RICHARDS, A. G. (1967). Sclerotization and the localization of brown and black colors in insects. *Zool. J. (Anat.)* **84**, 25–62.

RUTSCHKE, E. (1966). Submikroskopische Struktur schillernder Federn von Entenvögeln. *Z. Zellforsch. mikrosk. Anat.* **72**, 432–443.

SCHULTZ, T. D. & RANKIN, N. A. (1985). Developmental changes in the interference reflectors and colorations of tiger beetles (*Cicindela*). *J. exp. Biol.* **117**, 111–117.

SHELFORD, V. E. (1917). Color and color pattern mechanisms of tiger beetles. *Illinois. biol. Monogr.* **3**, 4.

SPRUNG, F. (1931). Die Flugeldecken der Carabidae. *Z. Morph. Ökol. Tiere* **24**, 435–490.

STEGMANN, F. (1930). Die Flugeldecken der Cicindelidae. Ein Beitrag zur Kenntnis der Insektcuticula. *Z. Morph. Ökol. Tiere* **18**, 1–73.

VAN WISSELINGH, C. (1914). Anwendung der in der organishen Chemie gebräuchlichen Reaktionen bei der phytomikrochemischen Untersuchungen. *Folia microbiol., Delft* **3**, 165–198.

WIGGLESWORTH, V. B. (1933). The physiology of the cuticle and of ecdysis in *Rhodnius prolixus* (Triatomidae: Hemiptera) with special reference to the function of the oenocytes and of the dermal glands. *Q. Jl microsc. Sci.* **76**, 269–315.

WIGGLESWORTH, V. B. (1972). *The Principles of Insect Physiology*. London: Chapman & Hall.

ZACHARUK, R. Y. (1972). Fine structure of the cuticle, epidermis, and fat body of larval Elateridae (Coleoptera) and changes acquainted with molting. *Can. J. Zool.* **50**, 1463–1487.

ZELAZNY, B. & NEVILLE, A. C. (1972). Quantitative studies on fibril orientation in beetle endocuticle. *J. Insect Physiol.* **18**, 1095–2122.